Research Article

For reprint orders, please contact: reprints@futuremedicine.com

Nanomedicine

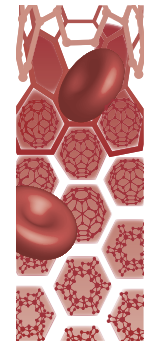

Dodecyl creatine ester-loaded nanoemulsion as a promising therapy for creatine transporter deficiency

Gabriela Ullio-Gamboa[1], Kenea C Udobi[2], Sophie Dezard[3], Marla K Perna[2], Keila N Miles[2], Narciso Costa[1], Frédéric Taran[3], Alain Pruvost[4], Jean-Pierre Benoit[5], Matthew R Skelton[2], Pascale de Lonlay[6] & Aloïse Mabondzo*[,1]

[1]Service de Pharmacologie et d'Immunoanalyse, CEA, Université Paris-Saclay, F-91191 Gif-sur-Yvette, France

[2]Department of Pediatrics, University of Cincinnati College of Medicine & Division of Neurology, Cincinnati Children's Research Foundation, Cincinnati, OH, USA

[3]Service de Chimie Bio Organique et de Marquage CEA, Université Paris-Saclay, F-91191 Gif-sur-Yvette, France

[4]Service de Pharmacologie et d'Immunoanalyse (SPI), Plateforme Smart-MS, CEA, INRA, Université Paris-Saclay, F-91191 Gif-sur-Yvette, France

[5]LUNAM Université-Micro et Nanomédecines Biomimétiques, F-49933 Angers, France, INSERM U1066, IBS-CHU, 4 rue Larrey, F-49933 Angers Cedex 9, France

[6]Centre de Référence des Maladies Héréditaires du Métabolisme de l'Enfant et de l'Adulte, Hôpital Necker-Enfants Malades, APHP, Université Paris Descartes, Imagine, INEM, Filière G2M, metabERN, Paris, France

*Author for correspondence: Tel.: +33 1 69081321; aloise.mabondzo@cea.fr

Creatine transporter (CrT) deficiency is an X-linked intellectual disability caused by mutations of CrT. **Aim:** This work focus on the preclinical development of a new therapeutic approach based on a microemulsion (ME) as drug delivery system for dodecyl creatine ester (DCE). **Materials & methods:** DCE-ME was prepared by titration method. Novel object recognition (NOR) tests were performed before and after DCE-ME treatment on *Slc6a8*$^{-/y}$ mice. **Results:** Intranasal administration with DCE-ME improved NOR performance in *Slc6a8*$^{-/y}$ mice. *Slc6a8*$^{-/y}$ mice treated with DCE-ME had increased striatal ATP levels mainly in the striatum compared with vehicle-treated *Slc6a8*$^{-/y}$ mice which was associated with increased expression of synaptic markers. **Conclusion:** These results highlight the potential value of DCE-ME as promising therapy for creatine transporter deficiency.

First draft submitted: 7 February 2019; Accepted for publication: 28 March 2019; Published online: 30 April 2019

Keywords: creatine • creatine transporter deficiency • dodecyl creatine ester • drug delivery • microemulsion • nasal administration • neurotherapeutics for CTD

Creatine transporter deficiency (CTD) is an X-linked inherited metabolic disorder caused by loss-of-function mutation in the *SLC6A8* gene encoding the creatine transporter (CrT). The CrT is responsible for the entry of creatine (Cr) into cells and mutations in CrT result in reductions of brain Cr. Individuals with CTD have moderate to severe intellectual disability, behavioral disorder such as attention deficit, hyperactivity disorder or autistic behavior and occasionally epilepsy [1–3]. CTD is a rare disorder, though it may be underdiagnosed due to the similarities between CTD and other autistic-like disorders. There are currently (October 2018) 383 cases of individuals with *SLC6A8* variants listed on a dedicated online database (https://databases.lovd.nl/shared/variants/SLC6A8). The estimated exome variant server database suggest that there are approximately 35,000 female CTD variants in the USA [4]. To date, there are no treatments available for CTD as oral creatine administration is ineffective. The primary role of Cr is to buffer energy levels in high energy consuming cells, particularly those of the brain, heart and muscle. In a reversible reaction catalyzed by Cr kinase, a phosphate group from ATP generated by oxidative phosphorylation or glycolysis is transferred to Cr to form pools of phospho-Cr. The phosphate group could then be transferred to ADP at the sites of ATP consumption, providing rapid energy replenishment. The importance of Cr in maintaining ATP levels is shown by the reduction of brain ATP in *Slc6a8*$^{-/y}$ mice [5]. The reductions in ATP could have wide implications for cellular function and may be responsible for several of the observed phenotype in

Future Medicine

CTD patients. Indeed, Cr and phospho-Cr have been linked to neuronal morphology and the uptake of glutamate into synaptic vesicles [5,6]. In addition to its role as energy reserve, creatine can protect against excitotoxicity as well as against β-amyloid toxicity *in vitro*. Creatine produced dose-dependent neuroprotective effects against (1-methyl-4-phenyl-1,2,3,6-tetrahydropyridine) MPTP toxicity reducing the loss of dopamine within the striatum and the loss of dopaminergic neurons in the substantia nigra [7,8]. Due to its neuroprotective effects, creatine is now in clinical trials for the treatment of Parkinson's disease. This neuroprotective and neuromodulatory effects that may be independent of its energetic role could contribute to the neurologic symptoms of CTD [7].

As the cause of CTD is obvious – the brain lacks Cr – therapeutic strategies should focus on increasing Cr and phospho-Cr stores in the brain. Improvements in cognitive ability and quality of life are achieved in individuals with disorders of Cr synthesis following Cr supplementation. However, the inability of Cr to cross the blood–brain barrier (BBB) without the functional CrT presents a unique challenge in CTD. In order to get Cr into the brain, the BBB must be circumvented or the brain must be stimulated to synthesize Cr itself. Since the Cr synthesis enzymes Arginine: Glycine Amidinotransferase (AGAT) and Glycine Amidinotransferase (GAMT) are expressed in the brain, few studies were conducted in which CTD patients were supplemented with Cr synthesis precursor's arginine, methionine and glycine [9]. There were no appreciable increases in brain Cr levels or cognitive ability in these patients though the combination therapy did halt the progression of symptoms in some patients. [10,11]. This would suggest that the only viable treatment strategy for CTD is to circumvent the BBB through Cr derivates or by masking the polar ends of Cr. The Cr mimetic cyclocreatine (cCr) is a planar molecule that can be phosphorylated/dephosphorylated by Cr kinase, though it should be noted that the reaction favors phospho-cCr over cCr. This makes cCr a poorer phosphate donor compared with Cr. Using *Camk2a-Cre,* mice lacking *Slc6a8* in forebrain neurons showed cognitive deficits compared with wild-type mice. These deficits were ameliorated following 9 weeks of cCr supplementation [12]. While this study shows promise, the limitations of cCr as a phosphate donor necessitate improved treatment strategies which focus on replacing the endogenous Cr in the brain. A possible treatment strategy for CTD is to use lipophilic Cr derivatives which could then be cleaved to Cr in the brain [13]. Based on structure–activity relationship, dodecyl creatine ester (DCE) is one of the most likely Cr derivatives to be incorporated into the brain [13]. Accordingly, DCE crossed brain endothelial cells and was able to diffuse through the *in vitro* rat primary cell-based BBB and into neurons. Increased Cr content was observed in fibroblasts from CTD patients incubated with DCE [14]. Together, this makes DCE an ideal leader molecule for *in vivo* testing. However, there is concern that degradation of DCE by somatic esterases would prevent a significant accumulation of Cr in the brain. Therefore, the development of an efficient drug delivery system is required. To address this, we developed an optimized microemulsion (ME) based on approved US FDA excipients to improve DCE delivery and membrane transport. The ME system may offer protection from chemical and enzymatic degradation [15,16]. Further, we utilized intranasal administration as it holds great potential for nose-to-brain drug delivery. The purpose of this study was to determine if this treatment strategy could increase brain Cr and improve cognitive function in ubiquitous *Slc6a8*$^{-/y}$ mice. These mice have significant cognitive deficits, as evidenced by poor spatial learning and memory, decreased novel object recognition (NOR) memory and reduced conditioned fear memory [17]. The results of this study show that short-term treatment of *Slc6a8*$^{-/y}$ mice with DCE either by intracerebroventricular or by IN administration of DCE-ME improved NOR performance. This suggests that DCE-ME could be a promising candidate for the treatment of CTD.

Materials & methods

Materials

DCE was synthesized as described previously [13]. Creatine monohydrate, creatine (methyl-D3) monohydrate (Cr-d3) and docosahexaenoic acid (DHA) were from Sigma (St Quentin-Fallavier, France). Glyceryl monolinoleate (Maisine® CC), highly purified diethylene glycol monoethyl ether (Transcutol® HP) were from Gattefossé (Nanterre, France). Purified water was from Milli-Q® Advantage A10 System (Merck Millipore, Fontenay-sous-Bois, France) and ammonium acetate from Prolabo VWR International (Fontenay-sous-Bois, France). All other chemicals and solvents were from Sigma–Aldrich (Saint-Quentin-Fallavier, France) and used without further purification.

Solubility study

The solubility of DCE in the ME components was determined by adding excess drug to 1 g of each selected oil, surfactant/co-surfactant or a mixture of them in Eppendorf® tubes. The tubes were maintained at 37 ± 1°C in a shaker (Thermomixer C, Eppendorf, Montesson, France) for 48 h to attain equilibrium. Samples were centrifuged

(Thermo Fisher Scientific, Villebon-sur-Yvette, France) at 20,000 *g* for 5 min and the supernatant was filtered through a 0.22 µm filter (Sartorius, Goettingen, Germany) and analyzed in triplicate by LC-MS/MS.

DCE loaded MEs

The optimized ME formulation comprised 63% w/w Transcutol® HP and 25% w/w of water. The oil concentration was maintained at 12% w/w and comprised DHA and Maisine® CC (2:1% w/w). The specified amount of DCE was first dissolved in the oil phase, and the excess of nonsolubilized drug was removed by centrifugation at 20,000 *g* for 5 min. Then, the surfactant was added to the oily phase with magnetic stirring at room temperature (Stuart CB162, Bibbly Scientific, Nemours, France). Finally, a fixed amount of distilled water was added dropwise to the above mixture and stirred continuously until transparent and homogeneous ME were produced.

Pseudo ternary phase diagram

Pseudo ternary phase diagrams of oil, surfactant and water were constructed using the water titration method [18] to determinate the feasibility domain for ME formation. Maisine® CC was blended with DHA (forming the oily phase) in fixed weight ratios (1:1 and 2:1). Oily phase and surfactant were mixed at room temperature (25°C) at predetermined ratios (w/w) and ultra-purified water was added dropwise to each oily phase-surfactant mixture with continuous magnetic stirring. After equilibrium, the samples were visually checked and determined as being clear transparent ME. The phase diagrams were plotted using Statgraphics Centurion 18 software (Statgraphics Technologies, VA, USA).

Physico-chemical characterization

The size distribution and surface charge of the prepared nanocarriers were analyzed using a Vasco Flex nanoparticle size analyzer (Cordouan Technology, Pessac, France). Sample suspensions were diluted in deionized water to ensure convenient scatter intensity on the detector. The average hydrodynamic diameter, the polydispersity index and the ζ potential were determined at 25°C in triplicate. The pH of the final formulation was measured using an Inolab pH730 (WTW, Weilheim, Germany).

Transmission electron microscopy

The morphology of ME was studied using an LVEM5 transmission electron microscope (Cordouan Technologies, Pessac, France). Before analysis, samples were diluted with ultrapure water (1:50) and an ELMO glow discharge system for EM grids was applied following the manufacturer's protocol.

Storage stability

The stability of all the formulations was evaluated under storage conditions for 15 days at 4–8° C. Three sets of parameters were assessed at different time points: macroscopic appearance (presence of aggregated, cream formation, changes in color); particle size, polydispersity index and ζ potential; and leakage of DCE from the formulation.

DCE quantification in ME formulation

Drug loading was determined after sample centrifugation at 20,000 *g* for 5 min in a Sorvall ST 16R Centrifuge (Thermo Scientific, Villebon-sur-Yvette, France). Three samples of supernatant were prepared by dissolution of an exact quantity of ME dispersion in acetonitrile-1% formic acid. Chromatography was performed using a binary pump LC-30AD (Shimadzu Nexera X2, Paris, France) with a 2.0 × 150 mm Uptisphere Diol HPLC column (UP6OH, Interchim, Montluçon, France). The mobile phase consisted of 0.1% formic acid solution (A) and acetonitrile containing 0.1% formic acid (B) in isocratic mode at 20/80 (A/B) with a flow rate of 0.4 ml/min. Analyte (10 µl) was injected onto the column placed in an oven at 40°C. The total runtime was 6 min. Detection was done by MS/MS (Finnigan TSQ Quantum Discovery with Xcalibur and LCquan softwares, Thermo) in positive electrospray mode. Spray voltage was 3.0 kV and sheath and auxiliary gas pressures were 50 and 20 (arbitrary units), respectively. The in-source CID energy was fixed at 12 V and capillary temperature was 350°C. Tube lens and collision energy values were optimized for DCE compounds. The standard curves showed linearity over a range of 10–1000 ng/ml.

Stability in brain homogenates.

The homogenates from WT mice were obtained using a VCX 130 Ultrasonic processor (Sonics, CT, USA) with a 60-s program with a net power output of 130 W. The DCE-ME was mixed with brain homogenate (dilution

10.2217/nnm-2019-0059

1:10) and the mixtures were incubated at 37°C in a Thermomixer C (Eppendorf, Montesson, France) with the shaker speed set at 900 rpm. At predetermined time points (0, 0.25, 0.5, 1, 2 and 3 h), 100 µl of samples were collected and the extraction protocol applied for Cr quantification was used. The quantifications in LC-MS/MS were carried out as described above for DCE-ME. All the samples were assayed in triplicate.

Animals

Slc6a8$^{-/y}$ mice were generated and genotyped in-house according to published studies [5,17,19]. These mice were generated on a C57Bl/6 J background and have been maintained on this background since their generation. For the IN treatment study, mice were assigned groups using a random-number table. No more than one mouse/group was used from a litter. All experimental protocols were approved by the CCRF Institutional Animal Use and Care Committee and the facility is IACUC-approved. The experiments were performed using 91 male mice of 18–25 weeks old. Male mice were used due to the X-linked nature of CTD. Mice were housed under standard experimental conditions: room temperature (20 ± 2°C); light/dark cycle (14 h light/10 h dark); water and food *ad libitum*, and kept in social groups of four mice per cage. To minimize circadian rhythm influence, all behavioral testing was performed between 0900 and 1300 h. After testing was completed, mice were sacrificed according to ethical guidelines.

DCE-intracerebroventricular treatment

Mice were deeply anesthetized, placed in a stereotaxic frame and fitted with an (intracerebroventricular) ICV cannula, which was fitted to catheter tubing (Brain Infusion Kit 3, Alzet). The coordinates for cannula placement to target the lateral ventricle were (from bregma): A/P = +0.3 mm; M/L = -1.0 mm; D/V = -3.0 mm. The cannula was primed with the treatment compound prior to implantation. The tubing was guided under the dorsal dermis and a port was created between the shoulder blades. Following recovery (24–48 h), *Slc6a8*$^{-/y}$ mice were treated once daily for 5 days with either DCE (0.02 mg/g bodyweight/day) or vehicle (VEH) while *Slc6a8*$^{+/y}$ mice were only treated with VEH. Mice were transferred to a holding room and a syringe with a blunt end needle was attached to the port and 20 µl of compound was infused at a rate of 1 µl/min.

IN administration of DCE-ME treatment

As there were no significant differences in NOR performance in the previous cohort, mice were randomized prior to assignment to treatment groups. Using a P10 micropipette, 6 µl of DCE-ME or VEH was placed in the nostril. The intracerebroventricular treatment (DCE)-ME (4 mg/g) or VEH was given twice bilaterally (24 µl total volume) for each dose for 10 days.

Novel object recognition

Mice were tested in the ANY-box apparatus (Stoelting Company, IL, USA). Testing began on the fifth day of treatment and concluded on the last day of treatment. First, mice were habituated to an empty arena (41 × 41 cm) for 2 days (10 min/day) and then habituated to two identical objects in the chamber (10 min/day) for the following 2 days. On the fifth day, animals were presented with two new identical objects until 30 s of cumulative observation time between the objects was obtained. Total 1 h later, memory was tested by presenting the animal with an identical copy of one of the familiar objects along with a novel object and tested identically to the familiarization trial. Time exploring the object was defined as entry into a 2-cm zone around the object. Performance was measured by an experimenter who was blinded to the treatment. A discrimination index was calculated where the time spent observing the novel object was subtracted from the time spent observing the familiar object and then divided by the total time of exploration.

Cr quantification in brain sample

Sample preparation

Before analysis, 0.2 g of water containing protease (5 X) and phosphatase (25 X) inhibitor cocktails (Roche, Boulogne-Billancourt, France) was added to different brain tissues to ensure that protein extracts did not degrade before analysis for targets of interest. The homogenates were obtained using a VCX 130 Ultrasonic processor (Sonics, CT, USA) with a 60-s program with a net power output of 130 W. From each brain sample, three separate aliquots were diluted 1:50 in the same cocktail mix and fortified with 10 µl of internal standard (IS) working solution containing 0.5 µg/ml creatine-d3 in water. Precooled 1% formic acid-acetonitrile (400 µl) was added and

each sample was vortex mixed for 30 s before 10 min of centrifugation at 10,000 *g*, 4°C in a Megafuge 16R Heraeus centrifuge (Thermo Fisher Scientific, Villebon-sur-Yvette, France). Sample supernatants were transferred to a clean set of tubes, placed in a 40°C water bath and evaporated to dryness under a 10–15 psi air stream in a TurboVap LV Evaporator (Biotage, Lund, Sweden). Sample residues were reconstituted in 200 µl of water/acetonitrile (50:50) 1% formic acid, vortex mixed for 30 s and centrifuged for 5 min at 10,000 *g* before transfer to vials.

Preparation of stock & working solutions

Stock solution containing 7.62 mM Cr was prepared in 1% formic acid solution. This stock solution was equally diluted in acetonitrile/water (95/5) 1% formic acid yielding eight working solutions (WS) from 2 to 45 µM for Cr. These working solutions were used to prepare the calibration standards (CS). Brain homogenate CSs and quality controls were prepared in duplicate by adding 10 µl of the corresponding WS to 90 µl of blank matrix and, after gentle vortexing, by adding 10 µl of the IS solution. This resulted in eight CSs containing Cr from 0.2 to 0.45 µM. Brain homogenate CSs and quality control samples were processed according to the previously described sample preparation method.

Chromatographic conditions & mass spectrometric parameters

The LC-MS/MS system consisted of a binary pump LC-30AD (Shimadzu Nexera X2) coupled to a triple quadrupole mass spectrometer TSQ Quantum Ultra (Thermo Scientific, Villebon-sur-Yvette, France). Analytes was ionized using electrospray ion source in positive mode. Chromatographic separation was achieved at 40°C via gradient elution of 10 mM buffer ammonium acetate (AA) pH 10 versus acetonitrile at a flow rate of 0.4 ml/min on an ACQUITY UPLC BEH Amide column (130 Å, 1.7 µm, 2.1 × 150 mm) with guard column provided by Waters (Saint-Quentin-en-Yvelines, France). The autosampler temperature was maintained at 4°C and the injection volume was 10 µl. The total runtime was 6 min. MS/MS conditions were established by infusing different diluted solutions of Cr, and Cr-d3, in the mass spectrometer in positive ionization mode. Data were acquired by MRM (multiple reaction monitoring) mode and the voltage ion spray was fixed at 3 kV. Quantification was performed using the transition m/z: 132.141→90.054 (CE = 15 V, tube lens = 60), lens = 57) for Cr.

Data analysis

The LCquan software (Thermo Electron Corporation) was used for method development, data collection and extracted peak integration. Linearity of the calibration curves was assessed by least-squared linear regression after normalization of the x- (concentration ratio of the analyte to the IS) and y-axis (peak area ratio of the analyte vs the IS) using the decimal logarithm. The method, which is intended for use during fundamental research, was validated using criteria adapted from the US FDA guidance. The amount of Cr was standardized to the amount of protein in each homogenate tissue by the Bradford technique following the manufacturer's instructions (Sigma–Aldrich, France).

Gene expression assessment by total RNA extraction & real-time quantitative PCR

The impact of brain Cr levels on gene expression of LTP biomarkers was determined by measuring mRNA levels of selected genes, *BDNF, C REB, PS95,* in brain tissues from treated and control *Slc6a8*$^{-}$/^{y} mice. Total RNA was extracted with QIAzol lysis reagent (Qiagen #79306) into Precellys lysing tubes and purified on RNeasy® Plus Universal minikit columns (Qiagen, Courtaboeuf, France #1062832). Briefly, brain tissues were lysed with 0.5 ml of QIAzol® reagent by pipetting. After addition of 100 µl of chloroform, mixtures were centrifuged at 10,000 *g* for 15 min at 4°C, supernatants mixed with 600 µl of 70% ethanol and loaded onto RNeasy® columns (Qiagen, Courtaboeuf, France). Total RNA was washed and eluted with RNase-free water according to the manufacturer's protocol and stored at -80°C. RNA concentration was measured spectrophotometrically at 260 nm in a NanoDrop 2000c (Thermo Scientific, Villebon-sur-Yvette, France; sample A260 nm/A280 nm ratios over 1.8 indicated reduced genomic DNA contamination). cDNAs were synthesized from 0.5 µg of total RNA with RT^{2} First Strand kit (Qiagen, Courtaboeuf, France #330411) according to the manufacturer's protocol and stored at -80°C. For qPCR, 9 ng of cDNA was mixed with 6.25 µl of iQ SYBR Green Supermix (Biorad #172-5124) and completed to 12 µl with milli-Q water. Mixes were loaded onto customized Hard-Shell® 96-Well PCR Plates (Bio-Rad #HSP9601) containing 0.3 µM of specific primers of each gene and the qPCR reactions were performed in a 7900HT Fast Real-Time PCR System (Applied Biosystems, Villebon-sur-Yvette, France) with the following cycle conditions: 95°C for 10 min, 40 cycles of 15 s at 95°C followed by 1 min at 60°C and finished by 30 s at 72°C.

10.2217/nnm-2019-0059

Table 1. Physico-chemical characterization of dodecyl creatine ester loaded-microemulsion.

Time (days)	Size (nm)	PI	ζ potential (mV)	Loading (mg/g)
0	137.9 ± 7.2	0.09	17.6 ± 2,3	3.9 ± 0.05
7	128.0 ± 12.5	0.06	16.8 ± 4.7	3.5 ± 0.2
15	148.8 ± 1.8	0.08	19.8 ± 0.7	3.0 ± 0.02

Data are shown as mean ± standard deviation (n = 3).
PI: Polydispersity index.

Threshold cycles (Ct) of target gene and cyclophilin A (Ppia as control housekeeping gene) were recorded and gene expression was calculated as $2^{-\Delta\Delta Ct}$ ($\Delta\Delta Ct$ = ΔCt treated - ΔCt control, ΔCt = Ct target - Ct Ppia). Specificity of PCR reactions was confirmed by melting curve analysis.

ATP assay

Slc6a8$^{-/y}$ and *Slc6a8*$^{+/y}$ mice were decapitated following brief isofluorane anesthesia. The five brain regions (olfactory bulb, cerebellum, hippocampus, cortex and striatum) were dissected and rapidly frozen in dry ice-cooled isopentane. Samples were weighed and homogenized in an equal volume of perchloric acid. ATP levels were analyzed using a commercially available fluorescence kit (Abcam Cambridge, MA, USA). ATP levels were normalized to tissue weight. Percent control levels were determined by dividing all samples by the mean of the *Slc6a8*$^{+}$/^{y} mice for the specific tissue studied.

Statistics

All statistical analyses were performed using GraphPad Prism software (Version 7.0). Experimental comparisons with multiple groups were analyzed using one-way ANOVA with either the two-stage linear step-up procedure of Benjamini, Krieger and Yekutieli used for *post hoc* analysis or with the Tukey's multiple comparison test for *post hoc* analysis. For comparison of two groups, two-tailed Student's or Mann–Whitney tests were performed and are noted in the figure captions. A p-value of 0.05 or less was considered statistically significant.

Results

Rational design & physico-chemical characterization of DCE-ME

We examined the design of versatile oil in water (O/W) ME prepared by the titration method and composed of US FDA-approved excipients which could enhance DCE solubility and thus improve its bioavailability. Furthermore, the lipophilic nature and the nanometric globular size of this system could account for the improvement in the absorption across the mucosal membranes [16].

The solubility of DCE was determined individually in a full lipids list at 2% w/w concentration. DCE had the highest solubility in glyceryl monolinoleate (Maisine® CC), and hence this lipid was employed in the preparation of ME. The criteria for selection of surfactant/cosurfactant were safety considerations, effective concentrations and preferably nonionic type. Among the tested surfactants and co-surfactants, the solubility of DCE was the highest in highly purified diethylene glycol monoethyl ether (DEGMEE; Transcutol® HP; 7.5 ± 0.5 mg/g) and thus this excipient was chosen for further studies. It should be pointed out that DEGME also acts as a permeation enhancer Figure 1 [20]. A summarizes the process of the rational design of our ME. Pseudoternary phase diagrams with different oil phase and surfactant compositions were constructed to determine the feasibility domain for ME formation (Figure 1B). DHA-rich oil, being a long chain triglyceride, exhibited poor penetration into the surfactant monolayer and showed a small ME region (data not shown). Thus, a combination of DHA with Maisine® CC (a mixture of mono-, di- and triglycerides of mainly linoleic and oleic acids) was evaluated at the ratios of 1:1 and 2:1, respectively. The ME region was identified as the area where clear and transparent formulations were observed and this area increased with increasing ratio of Transcutol® HP. However, at a surfactant concentration above 70%, the ME system formed a viscous gel. In fact, by increasing the surfactant concentration to a certain extent results in an enhanced water penetration into the oil droplets, causing interfacial disruption and ejection of oil droplets into the aqueous phase [21]. From the ternary plots, it was shown that the ME region at oil ratio DHA: Maisine®CC (2:1) was maximum when compared with 1:1, and thus this ratio was chosen and the oil content fixed at 12% in the final formulation. A stable monodispersion of about 130–150 nm particle size (IP ≤0.2) was obtained with pH of 4 ± 0.1 and positive ζ potential which accounts for its *in vivo* cellular uptake (Table 1). The presence of a relatively high ζ potential value led to stable nanodispersions and overcame the tendency of aggregation due to van der Waals

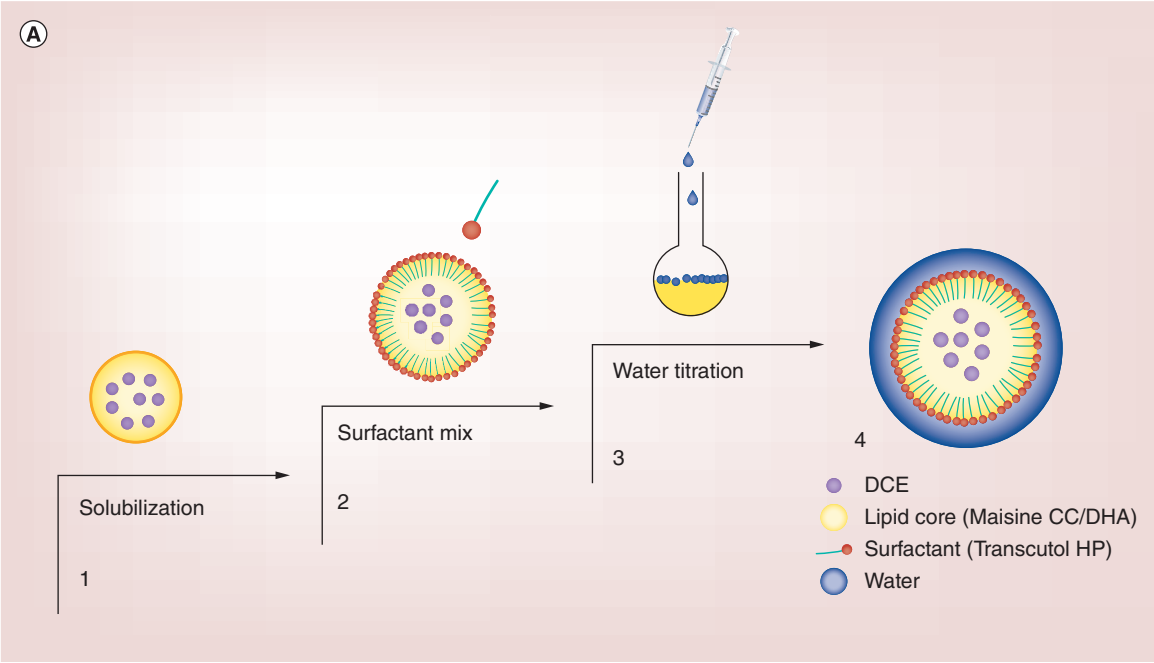

Figure 1. Rational design of DCE-ME strategy. (A) Schematic representation of microemulsion (ME) preparation. Solubilization of DCE in the inner lipid phase (Maisine®CC/DHA); surfactant addition (Transcutol® HP) under magnetic stirring; water titration to the previous mix and ME spontaneous formation; the final structure of the ME: a lipid inner phase in which DCE was previously solubilized surrounded by a surfactant shell and the external aqueous phase. **(B)** Ternary phase diagrams indicating o/w microemulsion region at different surfactant/oil/water mix ratios. Oil: Maisine®CC:DHA (1:1); oil: Maisine®CC:DHA (1:2). **(C)** Transmission electron microscopy micrograph of optimized DCE loaded ME.
DCE: Dodecyl creatine ester.

attraction forces. Moreover, nanosized droplets present greater surface area and high free energy, assuring faster and greater drug permeation through absorption barriers such as mucosal surfaces [22]. DCE was incorporated in ME with a loading of about 4 mg/g dispersion without the use of organic solvents. Moreover, no leakage of loaded DCE was observed after 15 days at storage conditions (4–8°C) (Table 1). The TEM photograph in Figure 1C also revealed the morphological characteristics of spherical oil droplets on the nanoscale in loaded ME.

To evaluate the stability of DCE-ME and its potential to turnover into Cr, we mimicked the *in vivo* conditions once the formulation reaches the brain. For this, we incubated DCE-ME in a brain mouse homogenate for 3 h at 37°C with gentle stirring and at different time points, we quantified the remaining DCE. We found that following 15 min of incubation, about 30% of the initial amount of DCE was found in the homogenate which means that DCE could be converted into Cr by the esterases from brain cells and available to restore the Cr pool. This hypothesis is supported by the increases in brain creatine content in the *Slc6a8*$^{-/y}$ mice model.

The remaining DCE could be attributed to the molecules that are deep in the core of the lipidic phase of the ME and thus delivered slowly. These results are in accordance with our previous finding concerning the conversion of DCE into Cr in human fibroblast cells [14].

Intracerebroventricular DCE treatment increases brain creatine content & rescues synaptic & cognitive deficits of *Slc6a8*$^{-/y}$ mice

Consistent with human CTD, *Slc6a8*$^{-/y}$ mice have reduced brain Cr content and cognitive deficits [17]. *Slc6a8*$^{-/y}$ mice also have reduced body mass and a near absence of Cr in most tissues, including the muscle [17,23]. This mouse model was used to test the efficacy of ICV-administered DCE compared with wild-type (WT) *Slc6a8*$^{+/y}$ mice used as control. It should be pointed out that DCE did not contribute to the mortality or morbidity of Slc6a8$^{-/y}$ mice. Prior to treatment, mice were tested in the NOR test. Consistent with previous findings, Slc6a8$^{-/y}$ mice showed object recognition deficits when compared with *Slc6a8*$^{+/y}$ mice (t_{31} = 2.35, $p < 0.05$). Mice were assigned to treatment groups by sorting animals based on discrimination index and alternating assignments between vehicle

10.2217/nnm-2019-0059

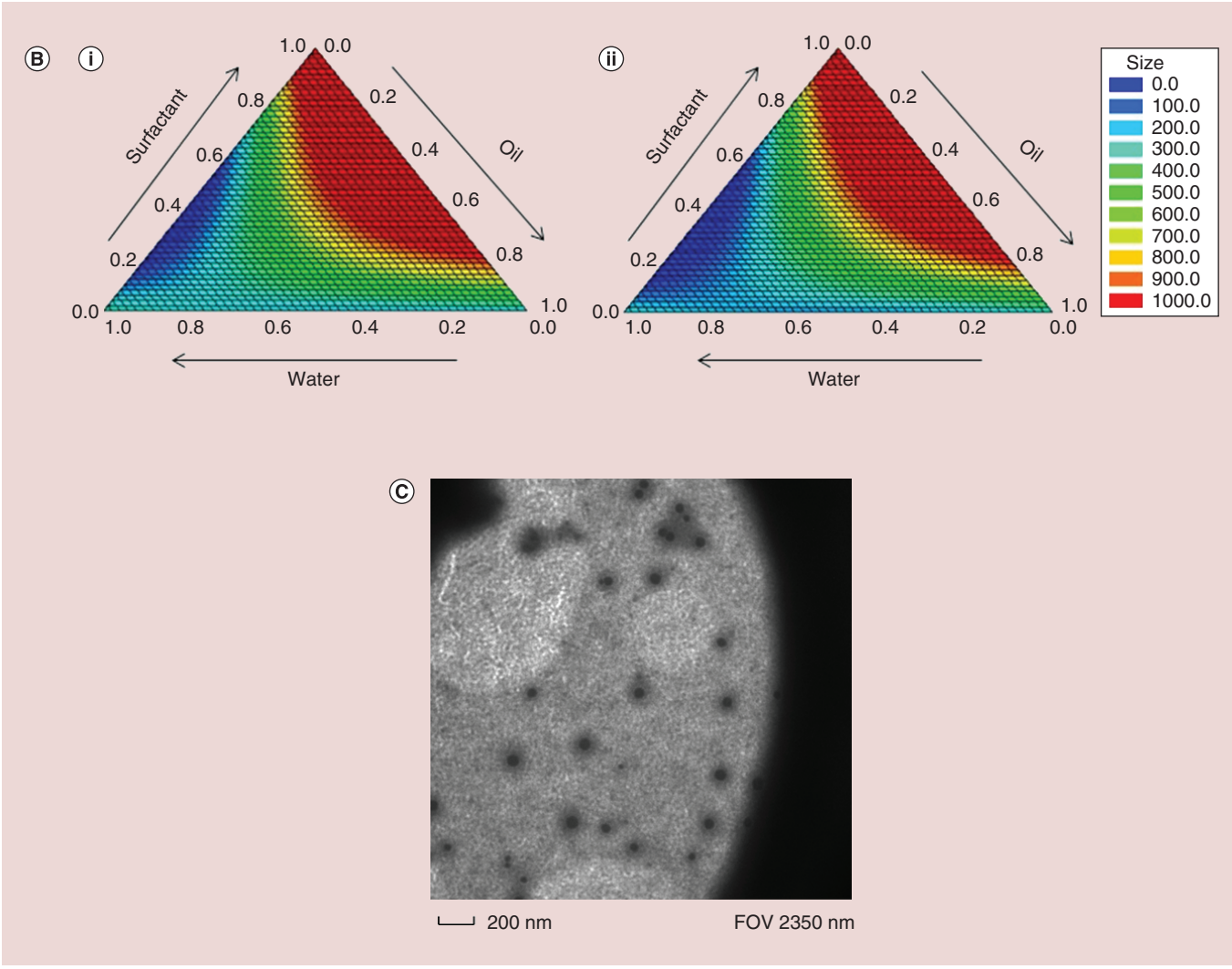

Figure 1. Rational design of DCE-ME strategy (cont.). (A) Schematic representation of microemulsion (ME) preparation. Solubilization of DCE in the inner lipid phase (Maisine®CC/DHA); surfactant addition (Transcutol® HP) under magnetic stirring; water titration to the previous mix and ME spontaneous formation; the final structure of the ME: a lipid inner phase in which DCE was previously solubilized surrounded by a surfactant shell and the external aqueous phase. **(B)** Ternary phase diagrams indicating o/w microemulsion region at different surfactant/oil/water mix ratios. Oil: Maisine®CC:DHA (1:1); oil: Maisine®CC:DHA (1:2). **(C)** Transmission electron microscopy micrograph of optimized DCE loaded ME.
DCE: Dodecyl creatine ester.

and treatment to avoid performance confounds. Accordingly, there were no pretreatment differences between *Slc6a8*$^{-/y}$ mice when analyzed by treatment group (t_{22} = 0.94, p = 0.353). Following ICV administration, there was a significant effect of group (F[2,21] = 7.035, p < 0.001) with *post hoc* analysis showing that DCE-treated *Slc6a8*$^{-/y}$ mice did not differ from control mice (p = 0.283). Vehicle-treated *Slc6a8*$^{-/y}$ mice showed reductions in object recognition as well as in Cr brain content in striatum, cortex, hippocampus and cerebellum tissues compared with both *Slc6a8*$^{+/y}$ and DCE-treated *Slc6a8*$^{-/y}$ mice (p < 0.05) (Figure 2A & B) even if there is some overlap in the lower quartile of the DCE-treated *Slc6a8*$^{-/y}$ versus the upper quartile of the Vehicle-treated *Slc6a8*$^{-/y}$ mice. The overall effect was that there was an increase in mean Cr levels. The results of the experiment show no toxic effect of DCE, suggesting the safety of this compound.

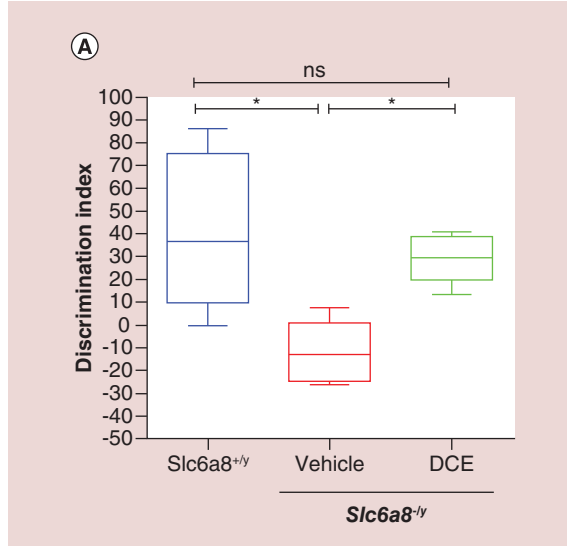

Figure 2. Improved object recognition memory in *Slc6a8*$^{-/y}$ mice and creatine content in different brain regions after intracerebroventricular treatment with dodecylcreatine ester. (A) Novel object recognition tests were conducted 1 h after familiarization in *Slc6a8*$^{-/y}$ and *Slc6a8*$^{+/y}$ (n = eight animal/group) mice treated for 5 days with vehicle or DCE. The discrimination index was calculated as the difference between new and familiar object exploration times divided by total time spent observing both objects. Experimental comparisons with multiple groups were analyzed using a one-way ANOVA with the false discovery rate method of Benjamini, Kreiger and Yekutieli used for *post hoc* analysis. Data are mean ± standard error of the mean. **(B)** Creatine content in different brain regions of Slc6a8$^{+/y}$ and Slc6a8$^{-/y}$ mice (n = 4) after intracerebroventricular administration of DCE measured by LC-MS/MS. Data are mean ± standard error of the mean. Mann–Whitney test.
*$p \leq 0.05$.
DCE: Dodecylcreatine ester.

Table 2. ATP levels in brain regions of Slc6a8-/y mice after nasal administration of dodecylcreatine ester-microemulsion.

Experimental conditions	ATP values (nMol/mg tissue wgt; mean ± SEM)				
	Striatum	Hippocampus	Olfactory bulb	Cortex	Cerebellum
Slc6a8$^{+/y}$	58.0 ± 7.3	270.5 ± 38.8	91.1 ± 13.6	47.1 ± 9.6	738.9 ± 99.4
Slc6a8$^{-/y}$ VEH	6.8 ± 1.4†,‡	13.1 ± 1.0†	52.8 ± 11.9†	26.6 ± 6.9	36.1 ± 4.5†
Slc6a8$^{-/y}$ DCE-ME	39.3 ± 10.3	12.0 ± 1.9†	52.3 ± 5.4†	27.8 ± 5.5	41.0 ± 4.6†

ATP levels were normalized to tissue weight. Percent control levels were determined by dividing all samples by the mean of the Crt $^{+/y}$ mice for the specific tissue studied. Data are shown as mean ± SEM (n = 6-8).
$^{\dagger}p < 0.05$ vs *Slc6a8*$^{+/y}$.
$^{\ddagger}p < 0.05$ DCE-ME vs vehicle.
DCE-ME: Dodecylcreatine ester-microemulsion; SEM: Standard error of the mean.

Intranasal administration of DCE-ME treatment improves object recognition learning in *Slc6a8*$^{-/y}$ mice

For the discrimination index, there was a main effect of group ($F[2,21] = 7.03$, $p < 0.01$). Multiple comparison analysis showed that DCE-ME treated *Slc6a8*$^{-/y}$ mice spent more time observing the novel object compared with vehicle-treated *Slc6a8*$^{-/y}$ mice ($p < 0.05$) but less time with the novel object compared with Slc6a8$^{+/y}$ mice ($p < 0.05$) (Figure 3). It is unlikely that changes in overall activity levels were responsible for the increase time spent with the novel object, as there was no effect of treatment on distance traveled in the arena during testing ($F[2,20] = 2.374$, $p = 0.12$; mean ± standard error of the mean: WT: 15.0 ± 1.8; VEH: 18.1 ± 1.8; DCE-ME: 20.3 ± 1.5). The rescue of cognitive deficit in *Slc6a8*$^{-/y}$ mice was associated with an increase of creatine in the different brain regions as shown by experiments carried out during DCE-ME optimization (Supplementary Figure 1). Interestingly, while Cr was increased in most of the brain regions, examined ATP was only increased in the striatum (Table 2). Since there is a wealth evidence that long-term potentiation (LTP) underlies certain form of memory [6], we were interested in the expression of LTP biomarkers after IN DCE-ME administration in *Slc6a8*$^{-/y}$ mice. While while *Bdnf* expression does not reached significance, a tremendous increased expression of *Psd95 and Creb* was observed following DCE-ME treatment of *Slc6a8*$^{-/y}$ mice (Figure 4A).

Discussion

CTD is an X-linked intellectual disability caused by mutations of creatine transporter leading to the perturbation of neuronal function. Based on our previous established relationship [13], DCE is one the most likely Cr derivatives diffusing passively through the cell membrane. These facts makes DCE as an ideal leader molecule for *in vivo* testing. In the present paper, we have demonstrated that following ICV administration DCE was able to diffuse through different brain regions; and turned into Cr in brain cells and improved cognitive function in *Slc6a8*$^{-/y}$ mice. The rescue of NOR deficits with a modest increase in Cr levels is in agreement with data from Kurosawa

10.2217/nnm-2019-0059

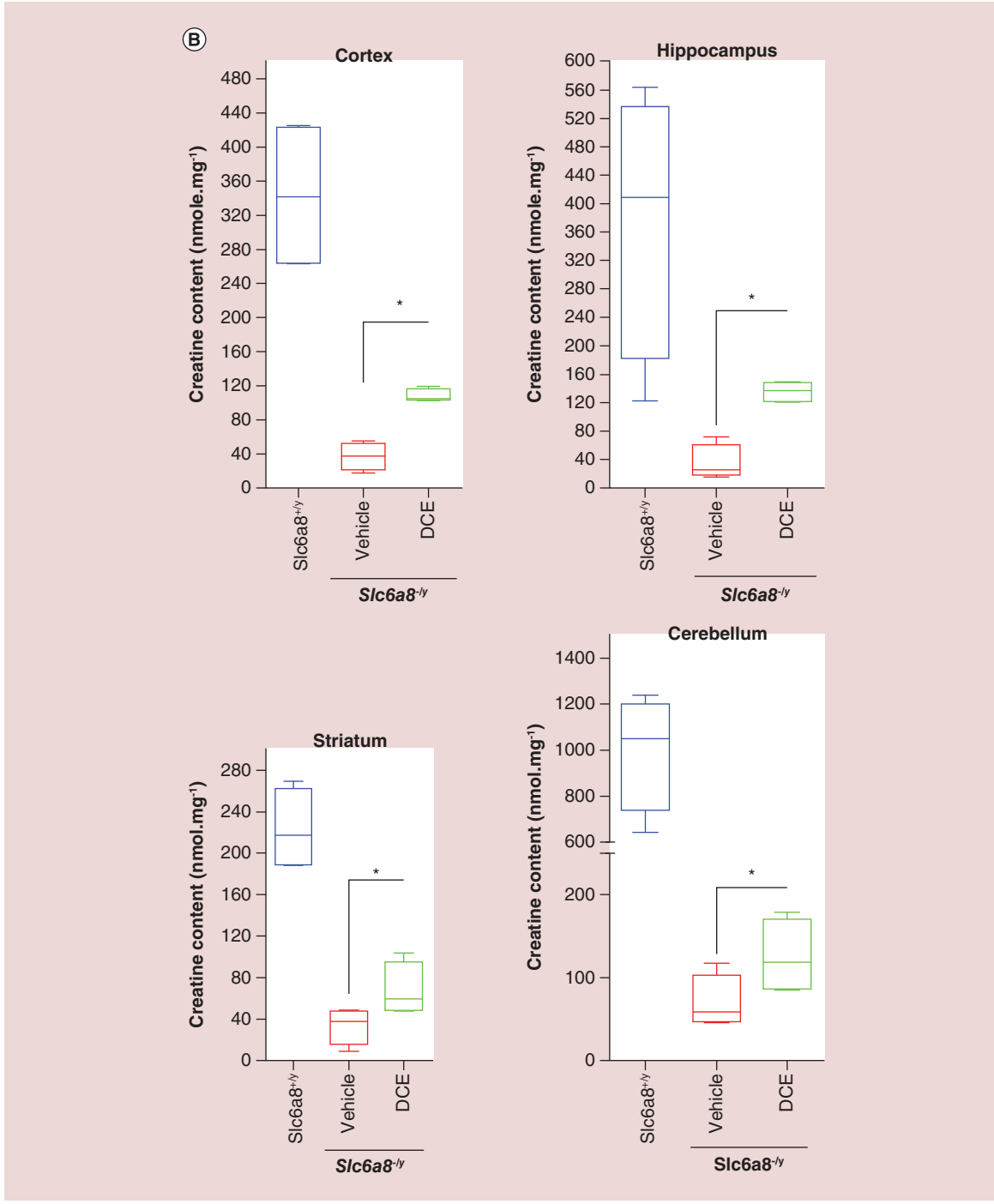

Figure 2. Improved object recognition memory in *Slc6a8*$^{-/y}$ mice and creatine content in different brain regions after intracerebroventricular treatment with dodecylcreatine ester (cont.). (A) Novel object recognition tests were conducted 1 h after familiarization in *Slc6a8*$^{-/y}$ and *Slc6a8*$^{+/y}$ (n = eight animal/group) mice treated for 5 days with vehicle or DCE. The discrimination index was calculated as the difference between new and familiar object exploration times divided by total time spent observing both objects. Experimental comparisons with multiple groups were analyzed using a one-way ANOVA with the false discovery rate method of Benjamini, Kreiger and Yekutieli used for *post hoc* analysis. Data are mean ± standard error of the mean. **(B)** Creatine content in different brain regions of Slc6a8$^{+/y}$ and Slc6a8$^{-/y}$ mice (n = 4) after intracerebroventricular administration of DCE measured by LC-MS/MS. Data are mean ± standard error of the mean. Mann–Whitney test.
*$p \leq 0.05$.
DCE: Dodecylcreatine ester.

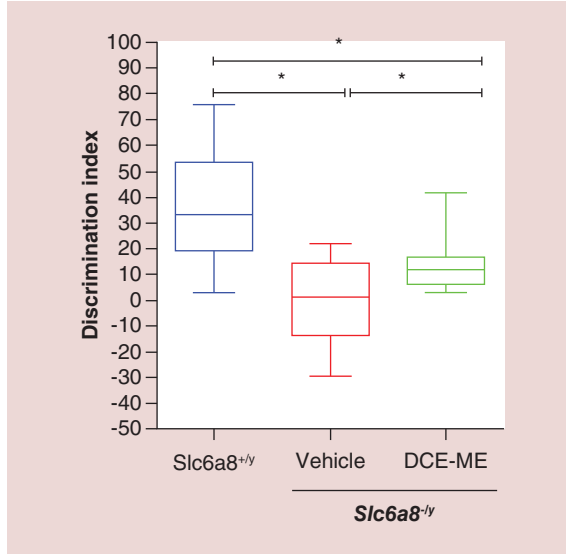

Figure 3. Improved object recognition memory in *Slc6a8*$^{-/y}$ mice after nasal administration of dodecylcreatine ester-microemulsion. Novel object recognition tests were conducted 1 h after familiarization in Slc6a8$^{-/y}$ and Slc6a8$^{+/y}$ (n = eight animal/group) mice before and after 10 days of intranasal treatment with vehicle or DCE-ME. Data were analyzed using one-way ANOVA with the false discovery rate method of Benjamini, Kreiger and Yekutieli used for *post hoc* analysis. Data are mean ± standard error of the mean.
*$p \leq 0.05$.
DCE-ME: Dodecylcreatine ester-microemulsion.

et al., who showed a restoration of NOR learning following cCr treatment [12]. The cCr levels in the brain of Slc6a8-deficient mice were approximately 50% of WT. Further, the total of Cr plus cCr in Slc6a8-deficient mice were approximately 25% of WT Cr + cCr. These facts suggest that restoring Cr levels to approximately 25% can preserve NOR learning. This is supported by data from the heterozygous Slc6a8 females, who have 50% of the brain Cr compared with WT mice and do not show NOR deficits [19].

For the pediatric clinical perspectives and keeping in mind that we expect in the future to treat patients showing moderate to severe intellectual disability, behavioral disorder such as attention deficit, hyperactivity disorder or autistic behavior, and occasionally epilepsy, we focused on the noninvasive therapeutic approach. We report in this paper and for the first time a new therapeutic approach based on a ME loaded with DCE for nasal delivery of DCE into the brain. This new formulation DCE-ME was well characterized. Due to its amphiphilic character, DCE was efficiently encapsulated into the optimized ME with an encapsulation efficiency of about 85%. The resulting delivery particles had a size around 150 nm and a positive charge stable which accounts for *in vivo* cellular uptake. Indeed, fatty acids present in Maisine® CC reduce ζ potential and suppress coalescence which provides a supplementary stabilizing effect for ME. Since our formulation was intended for IN administration, the inclusion of a biocompatible permeation enhancer such as DHA was of interest. This compound is also known for its role in neural function and is also involved in multiple brain functions including cell membrane fluidity, receptor affinity and modulation of signal transduction molecules [15,24,25].

Our ME drug delivery system was applied for the treatment of homozygous *SLC6A8*$^{-/y}$ mice following IN administration. Nasal administration of DCE-ME highlighted the interest of DCE-ME in improving cognitive deficit. The improvement of cognitive function is certainly due to the transport of DCE-loaded vesicles by either direct pathway through the olfactory bulbs or trigeminal nerve or either by the indirect pathway involving transport of DCE-loaded vesicles via lymphatic system. Once in the brain, DCE-loaded vesicles could be transported to various brain regions by extraneuronal, intraneuronal or transneuronal transport. The rescue of cognitive deficit in *Slc6a8*$^{-/y}$ mice was associated with an increase increasing of creatine in the different brain regions. These facts are in agreement with data from Kurosawa *et al.*, who showed a restoration of NOR learning following cCr treatment [12]. In addition, our data suggest that ATP-generated oxidative phosphorylation or glycolysis is transferred to Cr to form pools of phospho-Cr. The phosphate group can then be transferred to ADP at the sites of ATP consumption, providing a rapid energy replenishment. These results are in agreement with previous observations [5]. Interestingly, while Cr was increased in most of the brain regions examined, ATP was only increased in the striatum. While the mechanism that underlies this is unknown, it could reflect the different metabolic demands of neurons from each region. While the method used to collect tissue may not adequately represent the physiological levels of ATP, great care was taken to ensure that the tissue taken from each mouse was treated similarly; therefore, ATP hydrolysis should be equal in across subjects.

10.2217/nnm-2019-0059

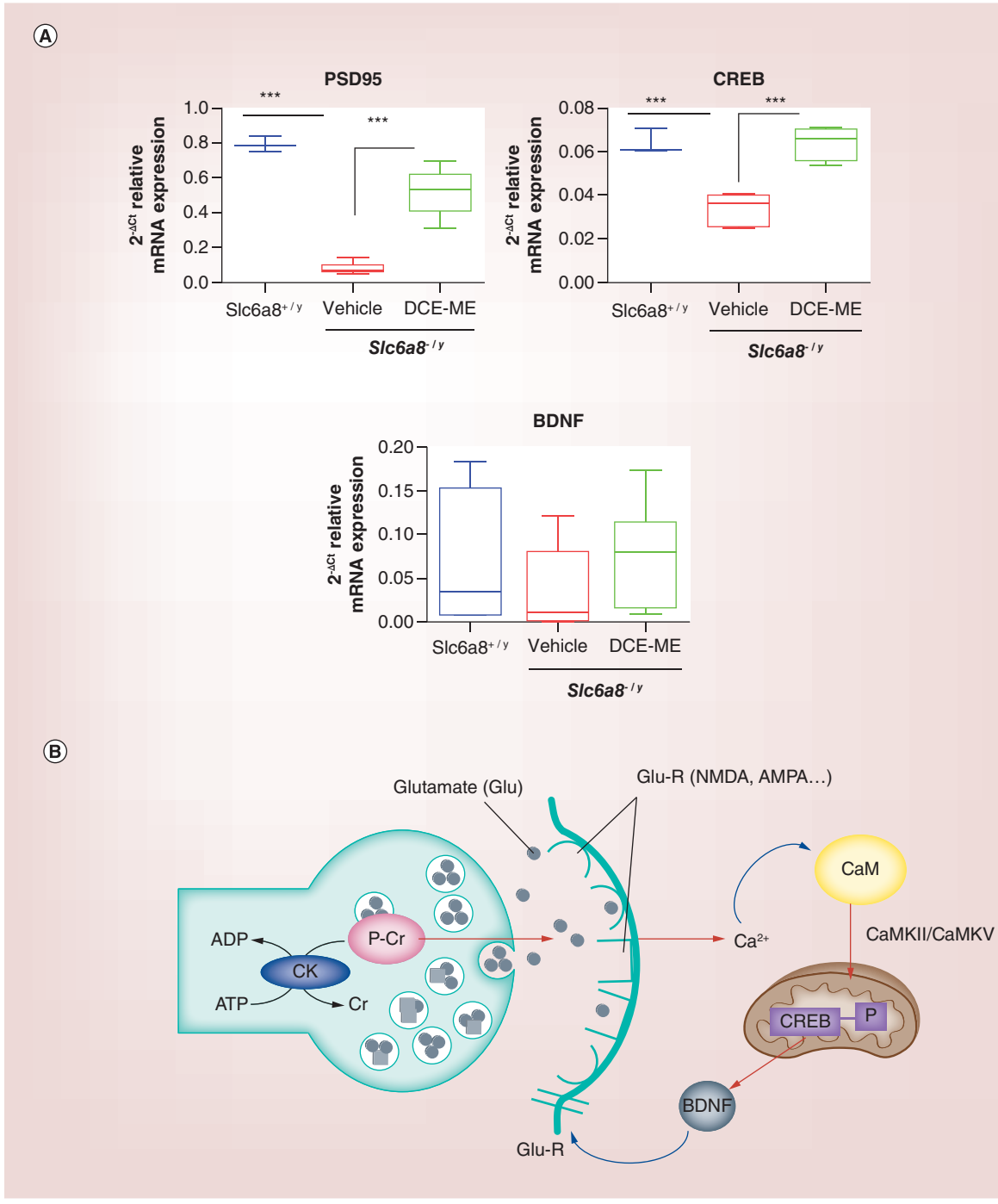

Figure 4. Nasal administration of dodecylcreatine ester-microemulsion rescue BDNF levels in the striatum of Scl6a8-/y mice. (A) Real-time PCR shows that in the striatum of *Scl6a8*$^{-/y}$ mice, ME increases *PSD95, CREB* and *BDNF* levels compared with nontreated *Scl6a8*$^{-/y}$ mice. One-way ANOVA with the Tukey's multiple comparison test for *post hoc* analysis were performed and ***$p < 0.001$ indicates significant differences between nontreated Scl6a8$^{-/y}$ mice and treated Scl6a8$^{-/y}$ mice or between Scl6a8$^{+/y}$ mice and nontreated Scl6a8$^{-/y}$ mice. Data are represent mean ± standard error of the mean (n = 3–6). **(B)** Schematic representation of regulation of synaptic markers in the striatum brain region implicated in novelobject recognition memory. The increased expression of Psd95, Creb and Bdnf participate in the restoration of cognitive function in the creatine transporter deficiency mice model.
***$p < 0.001$.
DCE-ME: Dodecylcreatine ester-microemulsion.

Literature highlighted the role of glutamate uptake in synaptic vesicles and through their action on postsynaptic receptors affect signal transduction processes involved in long-term potentiation (LTP) [5,6]. Increased expression of LTP biomarkers *Psd95, Creb* and *Bdnf* was observed following DCE-ME treatment of Slc6a8$^{-/y}$ mice. Figure 4B proposes a possible mechanism of action at the synaptic terminus in brain cells after DCE-ME IN administration in *Slc6a8*$^{-/y}$ mice. Our findings suggest that following the IN administration of our formulation, an increase of synaptic markers could be achieved in the synapsis terminals and thus improving the cognitive function of *Slc6a8*$^{-/y}$ mice. These results are in agreement with the role of LTP biomarkers in amelioration of learning memory and deficits in different animal models of neurodegenerative diseases [26,27].

There is no current treatment to improve the neurodevelopmental delays or increase creatine in brain in males with CTD. We report for the first time that DCE treatment using intranasal treatment of ME drug delivery system is an attractive approach to circumvent the BBB and to restore the cognitive function in homozygous *SLC6A8*$^{-/y}$ mice attributable to targeting Cr in brain cells. These results highlight the potential value of DCE-ME as promising therapy for CTD.

Future perspective

This study reports the first *in vivo* proof of concept for the treatment of the CTD by overcoming the BBB by the rational design of DCE nanoemulsion. Further studies are mandatory before evaluating the therapeutic efficiency of this strategy in CTD patients. We believe that the replenishment of creatine and consequently the improvement of cognitive function is due to the transport of DCE loaded vesicles by either direct pathway through the olfactory bulbs or trigeminal nerve or either by the indirect pathway involving transport of DCE-loaded vesicles via lymphatic system. Once in the brain, DCE-loaded vesicles could be transported to various brain regions by extraneuronal, intraneuronal or transneuronal transport. As perspective, experiments will be undertaken to formally confirm our hypothesis. In this context the incorporation of high sensitivity DCE-radiolabeled compound into the nano-engineered delivery system will help for *in vivo* pharmacokinetic profile of DCE-ME delivery system after nasal administration to Ko mice. DCE will be quantify by *ex vivo* radio-imaging, with or without MS coupling.

In addition, since CTD is a progressive metabolic disorder, we will perform a longitudinal investigation of neurochemical and behavioral readouts including investigations of synaptic brain plasticity biomarkers in animals of different ages intranasally treated with different DCE-ME doses. This will help for the determination of the therapeutic windows of our neurotherapeutics for the treatment of CTD.

Finally, toxicology reglementary studies will yield a strong therapeutic perspective for the treatment of CTD.

Summary points

- We have demonstrated that intracerebroventricular administration of dodecyl creatine ester (DCE) alone increase creatine levels in several brain regions of *Slc6a8*$^{-/y}$ mice.
- We have demonstrated that intracerebroventricular administration of DCE improve novel object recognition memory in *Slc6a8*$^{-/y}$ mice.
- We focus on the preclinical development of a new therapeutic approach based on a microemulsion (ME) as drug delivery system loaded with DCE (DCE-ME) on the treatment of *Slc6a8* knockout (*Slc6a8*$^{-/y}$) mice.
- DCE-ME formed monodispersed populations polydispersity index (PDI $\leq$0.2) with a mean size of around 150 nm and a positive charge surface.
- Due to its amphiphilic character, DCE was efficiently encapsulated into the optimized ME with an encapsulation efficiency of about 85%.
- Intranasal treatment with DCE-ME for 10 days improved novel object recognition performance deficits in *Slc6a8*$^{-/y}$ mice.
- These results highlight the potential value of DCE-ME as promising therapy for creatine transporter deficiency.
- Future pharmacology and toxicology studies will yield a strong therapeutic perspectives for the treatment of creatine transporter deficiency.

Supplementary data

To view the supplementary data that accompany this paper please visit the journal website at: https://www.futuremedicine.com/doi/suppl/10.2217/nnm-2019-0059

Author's contributions

Project administration: A Mabondzo. Conceptualization: A Mabondzo, P de Lonlay and J-P Benoit. Funding acquisition: A Mabondzo. Preformulation, formulation and stability evaluation: G Ullio-Gamboa. LC-MS/MS quantifications: A Pruvost and G Ullio-Gamboa. RT-PCR: N Costa. Drug synthesis: S Dezard and F Taran. *In vivo* experiments and acquiring data: MK Perna, KC Udobi, KN Miles and MR Skelton. Writing original paper: G Ullio-Gamboa, MR Skelton and A Mabondzo. All authors read and approved the final manuscript prior to submission.

Acknowledgements

We would like to thank AN Kokenge and ZI Abdulla for animal experiments as well as Gattefosse as suppliers for excipients.

Financial & competing interests disclosure

This work was supported by Fondation Le Jeune, Lucane Pharma and X-traordinaire (which is a patient group dedicated to intellectual deficiency rare diseases. Additional funding to MRS was provided by NIH (grant number: HD080910). The authors have no other relevant affiliations or financial involvement with any organization or entity with a financial interest in or financial conflict with the subject matter or materials discussed in the manuscript apart from those disclosed.

No writing assistance was utilized in the production of this manuscript.

References

Papers of special note have been highlighted as: •• of considerable interest.

1. Braissant O, Henry H, Béard E, Uldry J. Creatine deficiency syndromes and the importance of creatine synthesis in the brain. *Amino Acids* 40(5), 1315–1324 (2011).

•• **First description of a creatine pathophysiology**

2. Stockler S, Schutz PW, Salomons GS. Cerebral creatine deficiency syndromes: clinical aspects, treatment and pathophysiology. *Subcell. Biochem.* 46, 149–166 (2007).

3. Salomons GS, van Dooren SJ, Verhoeven NM *et al.* X-linked creatine-transporter gene (SLC6A8) defect: a new creatine-deficiency syndrome. *Am. J. Hum. Genet.* 68(6), 1497–1500 (2001).

•• **First description of a creatine pathophysiology.**

4. Desroches CL, Patel J, Wang P *et al.* Carrier frequency of guanidinoacetate methyltransferase deficiency in the general population by functional characterization of missense variants in the GAMT gene. *Mol. Genet. Genomics* 290(6), 2163–2171 (2015).

•• **First report describes the carrier fr carrier frequency of creatine transporter deficiency.**

5. Perna MK, Kokenge AN, Miles KN *et al.* Creatine transporter deficiency leads to increased whole body and cellular metabolism. *Amino Acids* 48(8), 2057–2065 (2016).

6. Xu CJ, Klunk WE, Kanfe JN, Xiong Q, Miller G, Pettegrew JW. Phosphocreatine-dependent glutamate uptake by synaptic vesicles: a comparison with atp-dependent glutamate uptake. *J. Biol. Chem.* 271(23), 13435–13440 (1996).

7. Fukumitsu K, Fujishima K, Yoshimura A, Wu YK, Heuser J, Kengaku M. Synergistic action of dendritic mitochondria and creatine kinase maintains ATP homeostasis and actin dynamics in growing neuronal dendrites. *J. Neurosci.* 35(14), 5707–5723 (2015).

8. Beal MF. Neuroprotective effects of creatine. *Amino Acids* 40(5), 1305–1313 (2011).

9. Bruun TUJ, Sidky S, Bandeira AO *et al.* Treatment outcome of creatine transporter deficiency: international retrospective cohort study. *Metab. Brain Dis.* 33(3), 875–884 (2018)

10. Valayannopoulos V, Boddaert N, Chabli A *et al.* Treatment by oral creatine, L-arginine and L-glycine in six severely affected patients with creatine transporter defect. *J. Inherit. Metab. Dis.* 35(1), 151–157 (2012).

•• **Reports on the lack of increases in brain Cr levels or cognitive ability in the creatine transporter deficiency patients.**

11. Jaggumantri S, Dunbar M, Edgar V *et al.* Treatment of creatine transporter (SLC6A8) deficiency with oral S-adenosyl methionine as adjunct to L-arginine, glycine, and creatine supplements. *Pediatr. Neurol.* 53(4), 360–363 (2015).

12. Kurosawa Y, DeGrauw TJ, Lindquist DM *et al.* Cyclocreatine treatment improves cognition in mice with creatine transporter deficiency. *J. Clin. Invest.* 122(8), 2837–2846 (2012).

13. Trotier-Faurion A, Dézard S, Taran F, Valayannopoulos V, De Lonlay P, Mabondzo A. Synthesis and biological evaluation of new creatine fatty esters revealed Dodecyl creatine ester as a promising drug candidate for the treatment of the creatine transporter deficiency. *J. Med. Chem.* 56(12), 5173–5181 (2013).

•• **First description of interset of dodecylcreatine-ester as promising drug for the treatment of creatine transporter deficiency.**

14. Trotier-Faurion A, Passirani C, Béjaud J *et al.* Dodecyl creatine ester and lipid nanocapsule: a double strategy for the treatment of creatine transporter deficiency. *Nanomedicine* 10(2), 185–191 (2015).

•• **First description of interset of a double strategy to overcome the blood–brain barrier and delivery of creatine into the brain.**

15. Shinde RL, Bharkad GP, Devarajan PV. Intranasal microemulsion for targeted nose to brain delivery in neurocysticercosis: role of docosahexaenoic acid. *Eur. J. Pharm. Biopharm.* 96, 363–379 (2015).

16. Callender SP, Mathews JA, Kobernyk K, Wettig SD. Microemulsion utility in pharmaceuticals: implications for multidrug delivery. *Int. J. Pharm.* 526(1–2), 425–442 (2017).

17. Skelton MR, Schaefer TL, Graham DL *et al.* Creatine transporter (CrT; Slc6a8) knockout mice as a model of human CrT deficiency. *PLoS ONE* 6(1), 1–10 (2011).

•• **Reports of a preclinical model of creatine transporter deficiency.**

18. Shah BM, Misra M, Shishoo CJ, Padh H. Nose to brain microemulsion-based drug delivery system of rivastigmine: formulation and *ex-vivo* characterization. *Drug Deliv.* 22(7), 918–930 (2015).

19. Hautman ER, Kokenge AN, Udobi KC, Williams MT, Vorhees CV, Skelton MR. Female mice heterozygous for creatine transporter deficiency show moderate cognitive deficits. *J. Inherit. Metab. Dis.* 37(1), 63–68 (2014).

20. Lin H, Gebhardt M, Bian S, Kwon KA, Shim CK, Chung SJ. Enhancing effect of surfactants on fexofenadine HCl transport across the human nasal epithelial cell monolayer. *Int. J. Pharm.* 330(1–2), 23–31 (2007).

21. Pouton CW. Formulation of self-emulsifying drug delivery systems. *Adv. Drug Deliv. Rev.* 25(1), 47–58 (1997).

22. Comfort C, Garrastazu G, Pozzoli M, Sonvico F. Opportunities and challenges for the nasal administration of nanoemulsions. *Curr. Top. Med. Chem.* 15(4), 356–368 (2015).

23. Udobi KC, Kokenge AN, Hautman ER *et al.* Cognitive deficits and increases in creatine precursors in a brain-specific knockout of the creatine transporter gene Slc6a8. Genes, Brain Behav. 17(6), 1–8 (2018).

•• **Reports on the evidence of the interest of creatine into the brain to rescue cognitive deficit in knockout creatine transporter deficiency mice.**

24. Muldoon MF, Ryan CM, Sheu L, Yao JK, Conklin SM, Manuck SB. Serum phospholipid docosahexaenonic acid is associated with cognitive functioning during middle adulthood. *J. Nutr.* 140(4), 848–853 (2010).

25. Yurko-Mauroa K, McCarthy D, Romb D *et al.* Beneficial effects of docosahexaenoic acid on cognition in age-related cognitive decline. *Alzheimers Dement.* 6(6), 456–464 (2010).

26. Fahnestock M, Marchese M, Head E *et al.* BDNF increases with behavioral enrichment and an antioxidant diet in the aged dog. *Neurobiol. Aging* 33(3), 546–554 (2012).

27. Neeper SA, Gómez-Pinilla F, Choi J, Cotman CW. Physical activity increases mRNA for brain-derived neurotrophic factor and nerve growth factor in rat brain. *Brain Res.* 726(1–2), 49–56 (1996).

10.2217/nnm-2019-0059